

# Performance of Sensitivity of Direct Detection Optical Receiver Incorporating MOSFET-Based Transimpedance-Type Amplifier

Abdulgaffar Swailim Muhawwis

Electrical & Electronic Department

College of Engineering

Thi-Qar University

## Abstract

Metal-Oxide-Semiconductor Field-Effect Transistors (MOSFETs) offer many advantages due to their low noise and high associated gain at microwave frequencies. Therefore, they are well suited to the amplifier requirements of broadband light-wave receivers, through providing a high dynamic range and wide bandwidths.

In this work, the performance of integrated optical receiver consisting of PIN-photodiode and MOSFET-based transimpedance type amplifier is analyzed. The effect of various device parameters on receiver performance is investigated in details. The simulation results show that the sensitivity ( $P_{sen}$ ) of an optical receiver is approximately constant if it is based on well-designed MOSFET.

**Keywords :** MOSFET, transimpedance amplifier, optical receiver, sensitivity, optical receiver noise, transconductance.

## المستخلص

توفر ترانزستورات الموسفيت عدة مزايا وذلك لما تمتاز به من كسب عالٍ وضوضاء قليلة في حزمة الترددات المايكروية. وللمزايا آنفة الذكر فإنها تكون ملائمة للمكبرات المستخدمة في المستلمات الضوئية من خلال توفيرها مدى ديناميكي عالي ضمن نطاق ترددي واسع. تم خلال هذا البحث تحليل أداء المستلمات الضوئية المكونة من ثنائي ضوئي نوع بي-آي-أن ومكبر إشارة مبني على أساس ترانزستورات الموسفيت. تم بحث تأثير تغير معالم الجهاز المذكور على الأداء بشكل تفصيلي. بينت نتائج المحاكاة بأن حساسية المستلم الضوئي تكون ثابتة تقريباً إذا تم تصميم ترانزستور الموسفيت بشكل جيد.

## 1. Introduction

The optical receiver is an optoelectronic device that recovers the transmitted electrical signal from the incident light wave signal. It is formed principally from a photo detector (photodiode or photoconductor), cascaded to a FET-based amplifier. Two photodiodes are mainly used in optical receiver design namely PIN photodiode and avalanche photodiode (APD). Theoretical sensitivities for both PIN/FET and APD/FET direct-detection receivers are shown in Figure (1) [1].

It is clear that the APD is attractive because of its superior sensitivity in APD/FET receivers. On the other hand, it is difficult to achieve significantly higher bandwidths in APD receivers, because of the avalanche build-up limitation, which could restrict the use of APDs in multigigabit systems [1]. PIN photodiodes have no such limitation, and bandwidth as high as 38 GHz has been reported [2]. Further, the PIN photodiode is preferred to APD because of the absence of excess multiplication noise.

MOSFETs based on AlGaAs/InGaAs structure offer many advantages due to their low noise [3], and high associated gain at microwave frequencies [1]. Therefore, they are well suited to the preamplifier requirements of broadband lightwave receivers.

It is also expected that the monolithic integration of optical and electronic components on the same chip will alternatively lead to ultra-high speed, high sensitivity, reliability, and low cost [4, 5]. Most of wide band optical receivers have been fabricated by integrating a PIN photodiode for light detection [3], and a transimpedance amplifier for electronic signal amplification and impedance matching [6].

In this work the performance of a monolithically integrated optical receiver consisting of a PIN photodiode and an MOSFET-based transimpedance type preamplifier is analyzed.

## 2. Optical receiver

### 2.1 Device description

In this analysis, the optical receiver considered consists of an InGaAs PIN photodiode integrated with a single gain stage transimpedance amplifier as shown in Figure (2). Such a preamplifier design provides a wide bandwidth and high dynamic range, which is defined as the range of input power levels over which the bit error rate is acceptable [7]. Note that all of the loads in the circuit are active to allow circuit integration with the other MOSFETs and to reduce device area and overall power dissipation. A conventional feedback resistor is replaced by a transistor ( $Q_3$ ) with an equivalent output resistance  $R_F$ . The use of a FET feedback may reduce parasitic shunt capacitance, thereby resulting in a wide bandwidth operation.

## 2.2 Receiver noise sources

The noise current of a receiver consists of low frequency (LF) noise, thermal noise in the feedback resistor, FET channel noise, and shot noise due to the leakage in the FET gate and the detector. These various noise contributions in an optical receiver are given by [5, 7]:

$$s_{sh} = \sqrt{2q(I_{Dark} + I_{leak})I_2B} \quad (1)$$

$$s_{ch} = 4pC_T B \sqrt{\frac{kT\Gamma I_3 B}{g_m}} \quad (2)$$

$$s_{LF} = 4pC_T B \sqrt{\frac{2kT\Gamma f_c I_f}{g_m}} \quad (3)$$

$$s_{th} = 2 \sqrt{\frac{kT I_2 B}{R_F}} \quad (4)$$

Here,  $\sigma_{sh}$ ,  $\sigma_{ch}$ ,  $\sigma_{LF}$ , and  $\sigma_{th}$  are the shot noise, channel noise, low frequency (LF) noise, and thermal noise standard deviations respectively,  $q$  is the electronic charge,  $k$  is the Boltzmann constant,  $g_m$  is the extrinsic transconductance,  $I_{Dark}$  is the PIN dark current,  $I_{leak}$  is the gate leakage current,  $B$  is the data bit-rate,  $T$  is the temperature,  $\Gamma$  is the MOSFET noise Figure ( $\approx 1.6$  [5]),  $f_c$  is the LF corner frequency, and  $C_T$  is the total front-end capacitance.  $C_T$  is calculated as:

$$C_T = C_{st} + C_{PD} + C_{GS} \quad (5)$$

where,  $C_{st}$  is the input stray capacitance,  $C_{PD}$  is the PIN diode capacitance, and  $C_{GS}$  is the MOSFET gate-source capacitance. Furthermore,  $I_f$ ,  $I_2$ , and  $I_3$  are effective receiver bandwidth integrals which depend on the transfer function of the circuit and the input and output waveforms. Here a raised cosine output pulse response of the receiver for a rectangular pulse shape, and a NRZ data format are assumed.

### 2.3 Receiver sensitivity

The receiver sensitivity is expressed in terms of minimum, time-averaged incident optical power ( $P_{sen}$ ), which can be detected for a given acceptable bit error rate (BER). Assuming Gaussian noise statistics, the sensitivity is given by [7]:

$$P_{sen} = \left( \frac{Qhf}{hq} \right) S_T \quad (6)$$

where,  $Q=6$  for  $BER=10^{-9}$ ,  $h$  is Planck constant,  $f$  is the frequency of the incident light,  $\eta$  is the overall efficiency in converting the incident optical power into a signal current, and  $\sigma_T$  is the total noise standard deviation which is defined as:

$$S_T = \sqrt{S_{sh}^2 + S_{ch}^2 + S_{LF}^2 + S_{th}^2} \quad (7)$$

Receiver sensitivity can be improved by decreasing the impedance at the interface. However, the low impedance at the PD-amplifier interface is highly non-optimal from a noise point of view, which, together with the intrinsic noise Figure of the amplifier, limits receiver sensitivity. The monolithic integration of transimpedance receiver is expected to be one of the facial ways to realize high sensitivity optoelectronic integrated circuits (OEICs) [8].

### 3. Transimpedance amplifier

The equivalent circuit of the PIN/transimpedance amplifier is shown in Figure.(3), where  $R_{in}$  is the input resistance of the amplifier,  $C_F$  is the stray capacitance of the feedback resistor  $R_F$ , and  $A$  is the amplifier voltage gain, and  $I_{ph}$  is the PIN diode photocurrent.

The response of the receiver is represented by the transimpedance  $Z_T$ , which is the ratio of the output voltage to the input photocurrent. The frequency dependence of  $Z_T$  is given by:

$$Z_T(f) = \frac{-AR_{in}R_F/[R_F + (1+A)R_{in}]}{1 + j \frac{2\pi f R_{in} R_F}{R_F + (1+A)R_{in}} [C_T + (1+A)C_F]} \quad (8)$$

Let  $Z_{T0}$  be the DC transimpedance, and  $f_{3dB}$  is the cutoff frequency (-3dB point), then:

$$Z_{T_o} = \frac{-AR_{in}R_F}{R_F + (1+A)R_{in}} \quad (9)$$

and

$$f_{3dB} = \frac{1}{2p \left[ \frac{R_{in}R_F}{R_F + (1+A)R_{in}} [C_T + (1+A)C_F] \right]} \quad (10)$$

Due to the use of equalization stage [8] in the receiver, the noise due to the intersymbol interference (ISI) is not considered [7]. So that, Eqn.(10) is useful in determining the bandwidth of the system.

In order to achieve the operation of the bit-rate (B) without equalization, the bandwidth of the preamplifier should be at least equal to the effective noise bandwidth of the receiver (12B). To accomplish this, RF must be adjusted such that f3dB is equal to the effective bandwidth. Let  $A \gg 1$  and  $AR_{in} \gg R_F$ , Eqn.(10) can be simplified as:

$$f_{3dB} = [2pR_F(C_F + C_T/A)]^{-1} \quad (11)$$

then

$$R_F = [2pI_2B(C_F + C_T/A)]^{-1} \quad (12)$$

This choice of RF ensures that thermal noise (Eqn.(4)) is not excessive, although it also implies a negligible intersymbol interference (ISI) noise. Figures(4a-4d) display the variation of different receivers noise sources as a function of B. Unless otherwise stated, the parameter values used in the simulation are listed in Table (1). The solid and dotted lines correspond, respectively, to the presence or absence of the equalization stage. It is clear that thermal and shot noises decrease in the absence of equalization. At B=10 Gbit/s, the thermal noise reduces to 0.075 of its value when equalization exists. This to be compared with 0.91 reduction for shot noise. So that, the thermal noise reduction is more important than that of the shot noise. The channel and LF noise behave in an opposite manner. However, at the same bit-rate, the channel noise and LF noise increase by factors of 1.4 and 2.08, respectively. As a result of not employing an equalization stage, the total noise current decreases to 0.107 of its value at equalization for 10 Gbit/s bit-rate. This is clear from Figure (5) where the total noise is plotted as a function of bit-rate.

In Figure (6), RF that satisfies the condition of negligible intersymbol interference is plotted as a function of the bit-rate. Note that  $R_F \approx 600 \Omega$  is required for B=10 Gbit/s. The dependence of receiver sensitivity on bit-rate is depicted in Figure (7). Note that Psen (in dBs)

decreases linearly with the logarithm of the bit-rate. For example, increasing B from 1 Gbit/s to 10 Gbit/s degrades the receiver sensitivity by 5 dB.

#### 4. Receiver performance

To calculate the performance of the optical receiver, a MOSFET with parameter values given in Table (2) are assumed. Other parameters used in this analysis are listed in Table (1). The MOSFET performance such as  $g_m$ ,  $C_{GS}$ , and  $C_{GD}$  are determined from expressions derived in [9].

Recall that the MOSFET capacitance and transconductance are functions of structure parameters of the device. Therefore, it is expected that the sensitivity of MOSFET-based receivers vary with transistor structure parameters. However, the simulation results reveal that this fact loses its importance when

- (i)  $C_{GS}$  is kept much lower than  $(C_{PD}+C_{st})$ ; or
- (ii) The total front-end capacitance to transconductance ratio ( $C_T/g_m$ ) is small. In other words, the operation speed of the MOSFET is much greater than the bit-rate.

Using the parameters listed in Tables (1) and (2), the PIN/MOSFET optical receiver sensitivity is plotted in Figure (8) as a function of CT for different values of gm. The results in this Figure indicate clearly that the receiver sensitivity is less affected by the variation of CT when CT is small and this effect is more pronounced when gm is high. For example,  $P_{sen}=-21.17$  dBm when CT is less than 500 fF and  $g_m=800$  mS. For the receiver under consideration, the values of CT and gm are 290 fF and 216 mS respectively. These values lead to -21.12 dBm receiver sensitivity. The simulation results indicate that  $P_{sen}$  is almost independent of the variation of MOSFET structure parameters. In fact,  $P_{sen}$  is almost independent of bias conditions (VGS and VDS) as shown in Table (3).

Figure (9a-9e) show, respectively, the effect of varying gate width (W), gate length (Lg) oxide layer thickens (di), semiconductor layer thickens (dd), and doping concentration (Nd) on receiver sensitivity. Investigating these Figures highlights the following facts:

- (i) For optical consideration, the optical receiver sensitivity is almost independent of gate width.
- (ii) There is a negligible degradation in  $P_{sen}$  ( $\approx 0.1$  dBm) as a result of increasing  $L_g$  from 20 to 100 nm.
- (iii) Increasing the oxide layer thickness from 1 to 100 Å improves the sensitivity by only 1 dB.

- (iv)  $P_{sen}$  remains almost unchanged by increasing the semiconductor layer thickness from 10 to 130 Å.
- (v) There is no remarkable dependence of  $P_{sen}$  on the doping concentration of the MOSFET semiconductor layer doping ( $N_d$ ).

To improve the receiver sensitivity slightly, the source resistance ( $R_s$ ) must be minimized since the intrinsic transconductance, which inversely proportional to the total noise current, increases with minimizing  $R_s$ . Figure (10) depicts the effect of  $R_s$  on receiver sensitivity. Reducing  $R_s$  from 30  $\Omega$  to 0  $\Omega$  improves the  $P_{sen}$  by only 0.3 dB.

## 5. Conclusion

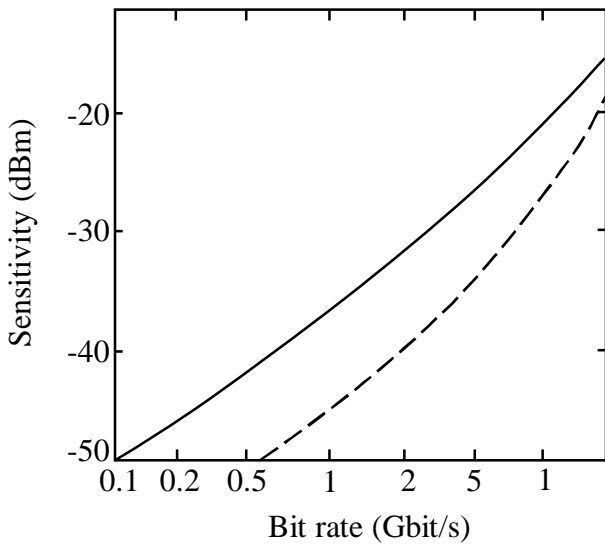
We analyze the performance optical receiver consisting of PIN-photodiode and MOSFET-based transimpedance type amplifier by investigating the effect of various device parameters on receiver performance. The simulation results show that the sensitivity ( $P_{sen}$ ) of an optical receiver approximately independent of gate width, degrade negligibly with the increase of the gate length, enhanced with the increase of oxide layer thickness, and approximately it has no change with semiconductor layer thickness and doping concentration.

## 6. References

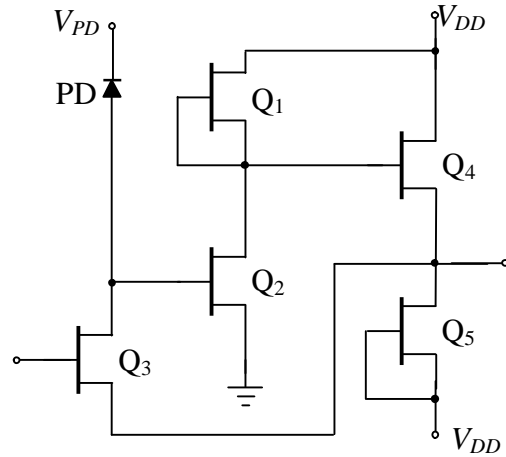
- [1] C. H. Chen and M. J. Deen, Aug. 2002, "Channel Noise Modeling of Deep Submicron MOSFETs," IEEE Trans. Electron Devices, vol. 49, pp. 1484–1487.
- [2] H. Shin, J. Jeon and S. Kim, September, 2006 "Analytical Thermal Noise Model of Deep Submicron MOSFETs," Journal of Semiconductors Technology and Science, vol. 6, No. 3.
- [3] B. Claflin, E. R. Heller, and B. Wenningham, May 18th-21st, 2009, "Accurate Channel Temperature Measurement in GaN-based HEMT Devices and its Impact on Accelerated Lifetime Predictive Models," CS MANTECH Conference, Tampa, Florida, USA.
- [4] Claudiu AMZA, Ovidiu-George PROFIRESCU, Ioan CIMPIAN, Marcel D. PROFIRESCU, 2008, "Monti Carlo Simulation of a HEMT Structures," Proceedings of The Romanian Academy of The Romanian Academy, Volume 9, Number 2.
- [5] Mustafa EROL, "Effect of Carrier Concentration Dependant Mobility on the Performance of High Electron Mobility Transistors," Turk J Phy, 25 (2001), 137 - 142.

- [6] Wen-Chau Liu, Wen-Lung Chan, Wen-Shiung Lour, Kuo-Hui Yu, Chin-Chuan Cheng, and Shiou-Yinh Cheng, 2001 , “Temperature-dependence investigation of a high performance inverted delta-doped V-shaped GaInP/InxGa1-xAs/GaAs pseudomorphic high electron mobility transistor,” IEEE Trans. Electron Devices, vol. 38, no. 7, pp. 1290-1296,.
- [7] D. C. W. Lo, and S. R. Forrest ,June 1989, “Performance of In<sub>0.53</sub>Ga<sub>0.47</sub>As and InP junction field effect transistors for optoelectronic integrated circuits. II. Optical receiver Analysis,” Journal of Lightwave Technology, Vol. 7, No. 6, pp. 966-971.
- [8] Alok Kushwaha, Manoj Kumar Pandey, Sujata Pandey, and A. K. Gupta, September 2005 ,“Analysis of 1/f Noise in Fully Depleted n-channel Double Gate SOI MOSFET,” Journal of Semiconductor Technology and Science, Vol.5, No.3.
- [9] R. S. Fyath, and H. N. Wazeer, 2002, "Performance Analysis of High Electron-Mobility Transistor for Optical Receiver," M. Sc. Thesis, University of Basrah, College of Engineering, Basrah, Iraq.

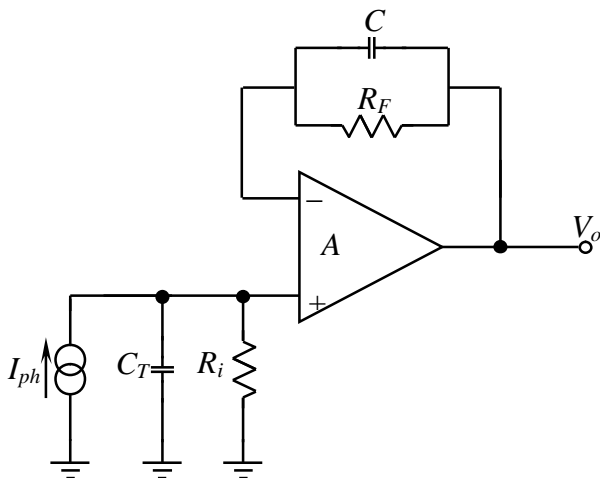




Figure(1). Receiver sensitivities versus bit-rate for PIN/FET (solid line) and APD/FET (dotted line) direct-detection receivers.



Figure(2). Circuit diagram of a transimpedance optoelectronic integrated circuit (OEIC) optical receiver.



Figure(3). Equivalent circuit of the Amplifier of Figure(2).

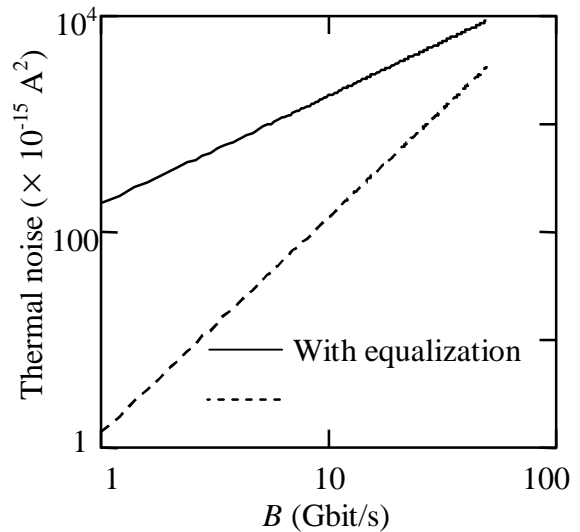


Figure (4a). Variation of thermal noise as a function of B for BER of  $10^{-9}$ .

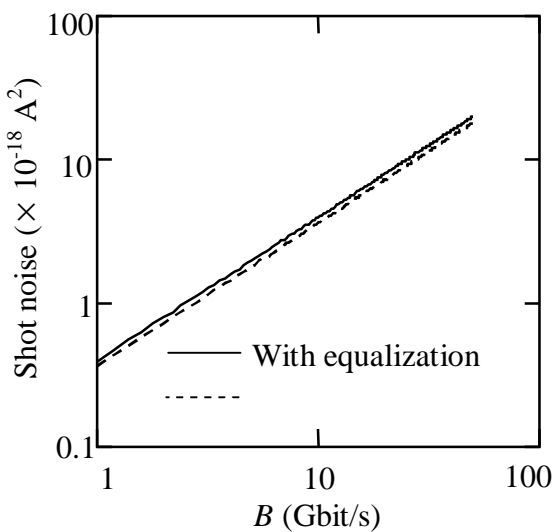


Figure (4b). Variation of Shot noise as a function of B for BER of  $10^{-9}$ .

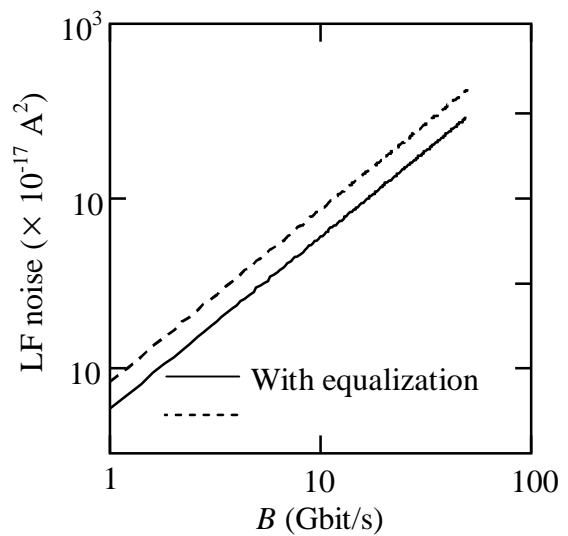


Figure (4c). Variation of LF noise as a function of B for BER of  $10^{-9}$ .

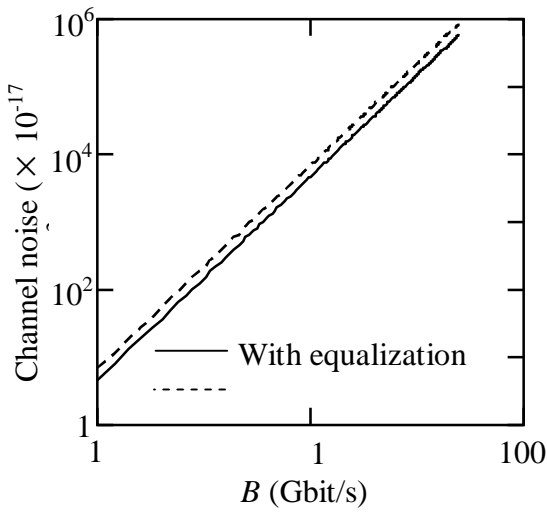


Figure (4d). Variation of Channel noise as a function of  $B$  for BER of  $10^{-9}$ .

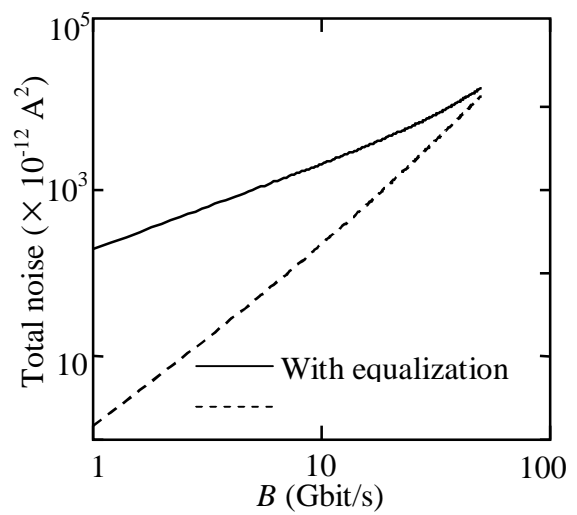


Figure (5). Total noise as a function of bit-rate for BER of  $10^{-9}$ .

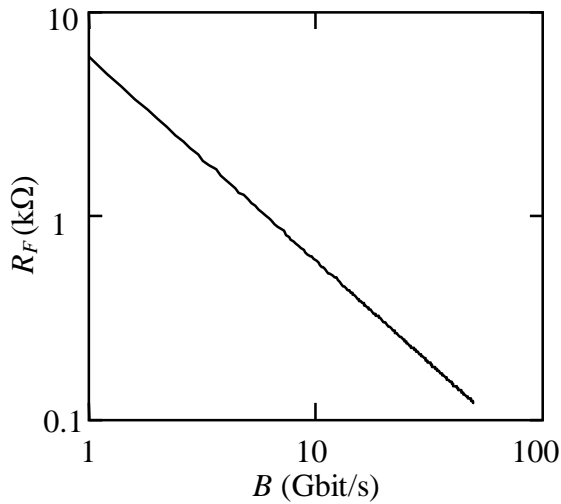


Figure (6). Feedback resistance satisfying the condition of negligible ISI noise as a function of the bit rate.

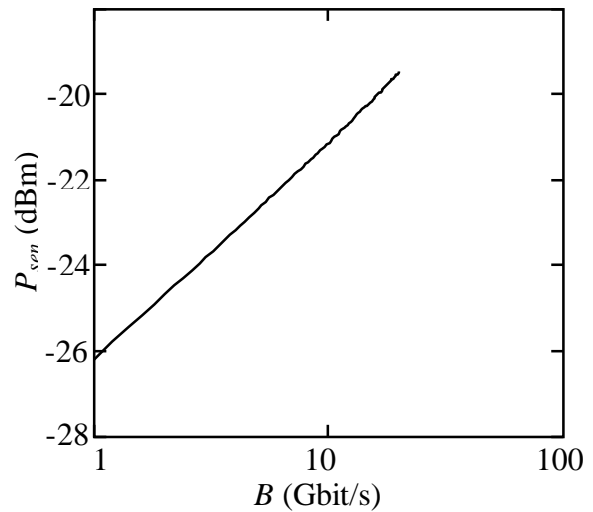
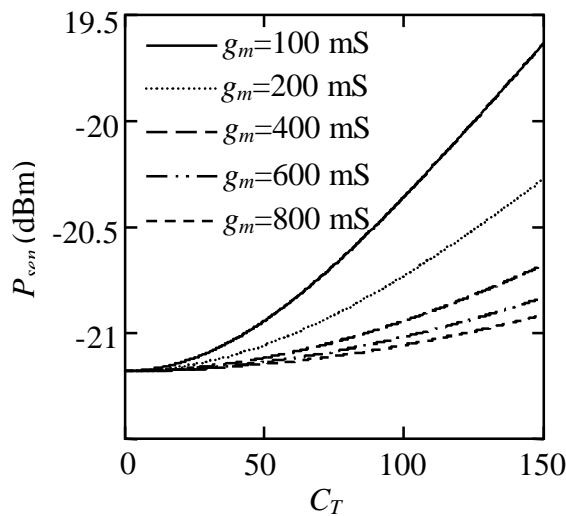
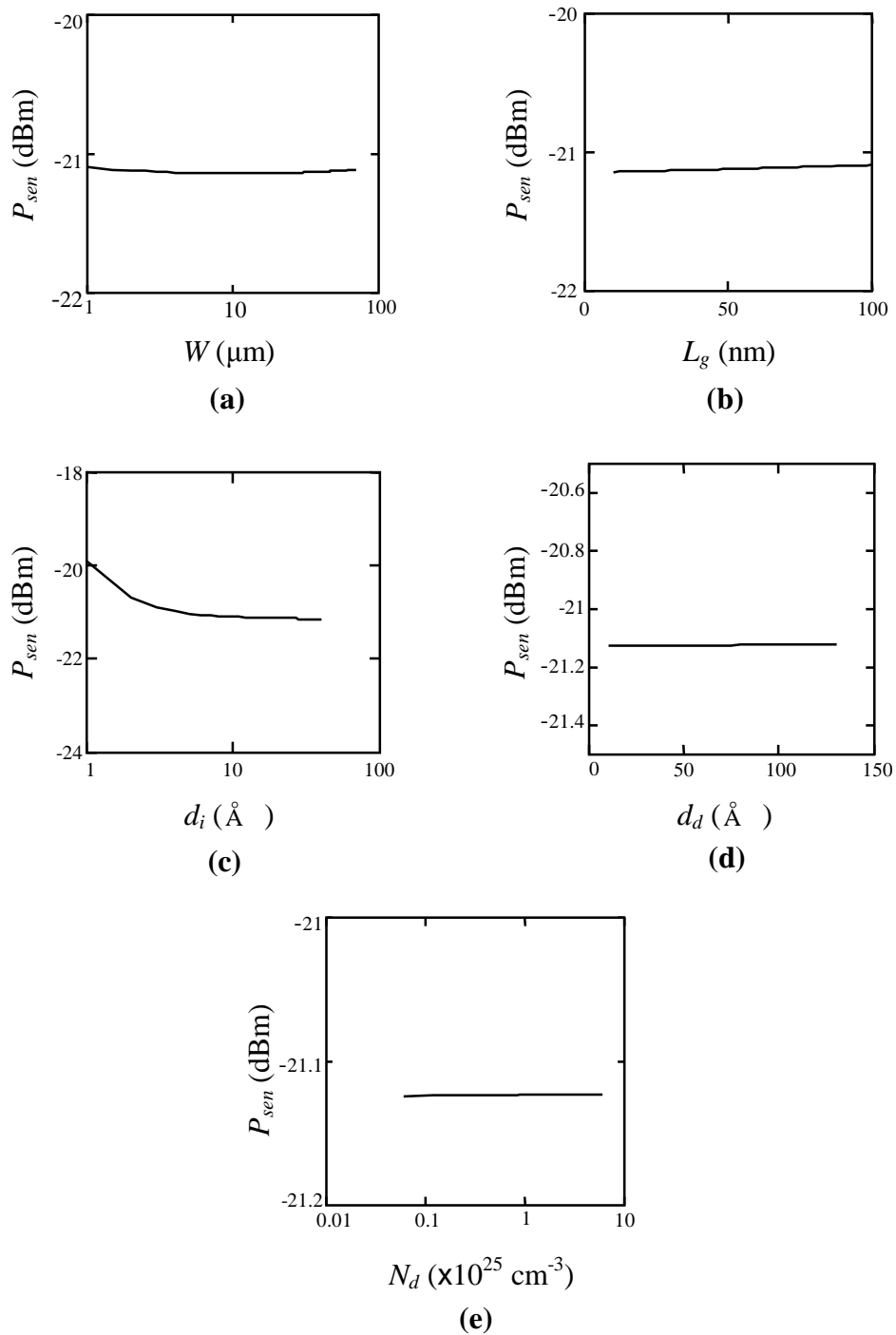


Figure (7). Receiver sensitivity as a function of data bit-rate.



Figure(8). Receiver sensitivity as a function of the total front-end capacitance ( $C_T$ ) for different values of extrinsic transconductance ( $g_m$ ).



**Figure (9). Effect of (a) gate width, (b) gate length, (c) undoped layer thickness, (d) doped layer thickness, and (e) doping concentration on receiver sensitivity.**

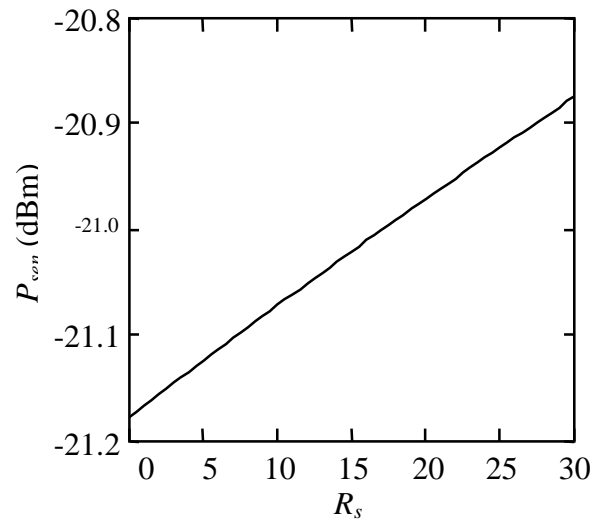


**Figure (10). Receiver sensitivity as a function of source resistance.**

**Table (1). Receiver parameters values used in the simulation.**

Parameter	Value	Unit
$Q$	6	-
$I_2$	0.55	-
$I_3$	0.085	-
$I_f$	0.12	-
$I_{dark}$	2	nA
$J_{leak}$	10	mA/cm <sup>2</sup>
$f_c$	25	MHz
$\lambda$	1.55	$\mu\text{m}$
$\Gamma$	1.6	-
$\eta$	0.85	-
$C_{PD}$	125	fF
$C_{st}$	125	fF
$B$	10	Gbit/s

**Table ( 2). MOSFET parameters used in the simulation.**

Parameter	Value	Unit
$L_g$	50	nm
$W$	50	$\mu\text{m}$
$d_i$	20	$\text{\AA}$
$d_d$	80	$\text{\AA}$
$\mu$	12800	$\text{cm}^2/\text{Vs}$
$v_{sat}$	$280 \times 10^7$	$\text{Cm/s}$
$\epsilon_r$	12.1	-
$N_d$	$6 \times 10^{18}$	$\text{cm}^{-3}$
$V_{off}$	-0.017	V
$R_s$	1.0	$\Omega$
$R_d$	1.0	$\Omega$

**Table (3). Receiver sensitivity (dBm) as a function of  $V_{DS}$  and  $V_{GS}$ .**

	$V_{GS}=0.2 \text{ V}$	$V_{GS}=0.3 \text{ V}$	$V_{GS}=0.5 \text{ V}$
$V_{DS}=0.5 \text{ V}$	-19.1218	-19.1225	-19.1231
$V_{DS}=1.0 \text{ V}$	-19.1219	-19.1226	-19.1232
$V_{DS}=1.5 \text{ V}$	-19.1220	-19.1227	-19.1233
$V_{DS}=2.0 \text{ V}$	-19.1220	-19.1228	-19.1234